3rd Micro and Nano Flows Conference
Thessaloniki, Greece, 22-24 August 2011

3D Modelling of Angiogenesis and Vascular Tumour Growth

Holger PERFAHL [1,*], Helen M. BYRNE [2], Tingan CHEN [3], Veronica ESTRELLA [3], Tomás ALARCÓN [4], Alexei LAPIN [1], Robert A. GATENBY [3], Robert J. GILLIES [3], Mark C. LLOYD [3], Philip K. MAINI [5,6], Matthias REUSS [1], Markus R. OWEN [7]

* Corresponding author: Tel.: ++49 (0)711 68565036; Fax: ++49 (0)711 685; Email: holger@perfahl.org
1 Center Systems Biology, University of Stuttgart, Germany
2 OCCAM and Department of Computer Science, University of Oxford, United Kingdom
3 H. Lee Moffitt Cancer Center and Research Institute, Tampa, United States of America
4 Centre de Recerca Matemàtica, Campus de Bellaterra, Barcelona, Spain
5 Centre for Mathematical Biology, Mathematical Institute, University of Oxford, United Kingdom
6 Department of Biochemistry, Oxford Centre for Integrative Systems Biology, University of Oxford, United Kingdom
7 Centre of Mathematical Medicine and Biology, School of Mathematical Sciences, University of Nottingham, United Kingdom

Keywords: Multiscale Modelling, Angiogenesis, Vascular Tumour Growth

Angiogenesis marks an important turning point in the growth of solid tumours. Avascular tumours rely on diffusive transport to supply them with the nutrients they need to grow and, as a result, they typically grow to a maximal size of several millimetres in diameter. Growth stops when the rate at which nutrient-starved cells in the tumour centre die balances the rate at which nutrient-rich cells on the tumour periphery proliferate. Under low oxygen, tumour cells secrete angiogenic growth factors that stimulate the surrounding vasculature to produce new capillary sprouts that migrate towards the tumour and the new vessels increase the supply of nutrients to the tissue, enabling the tumour to continue growing and to invade adjacent healthy tissue. At a later stage small clusters of tumour cells may enter the vasculature and be transported to remote locations in the body, where they may establish secondary tumours and metastases.

In more detail, the process of angiogenesis involves degradation of the extracellular matrix, endothelial cell migration and proliferation, capillary sprout anastomosis, vessel maturation, and adaptation of the vascular network in response to the blood flow. Angiogenesis is initiated when hypoxic cells secrete tumour angiogenic factors (TAFs), such as vascular endothelial growth factor (VEGF). The TAFs are transported through the tissue by diffusion where they stimulate the existing vasculature to form new sprouts. The sprouts migrate through the tissue, responding to spatial gradients in the TAFs by chemotaxis. When sprouts connect to other sprouts or to the existing vascular network via anastomosis, new vessels arise. The diameter of perfused vessels changes in response to a number of biomechanical stimuli such as wall shear stress and signalling cues such as VEGF. Angiogenesis persists until the tissue segment is adequately vascularised. On the other hand, vessels which do not sustain sufficient blood flow will regress and be pruned from the network.

The presented computational model describes the spatio-temporal dynamics of tumour growth in a vascular host tissue. Cells are represented as individual entities (agent-based approach) each with their own cell cycle and subcellular-signalling machinery. Nutrients are supplied by a dynamic vascular network, which is subject to remodelling and angiogenesis. The interactions between the different modules are depicted in Figure 1.

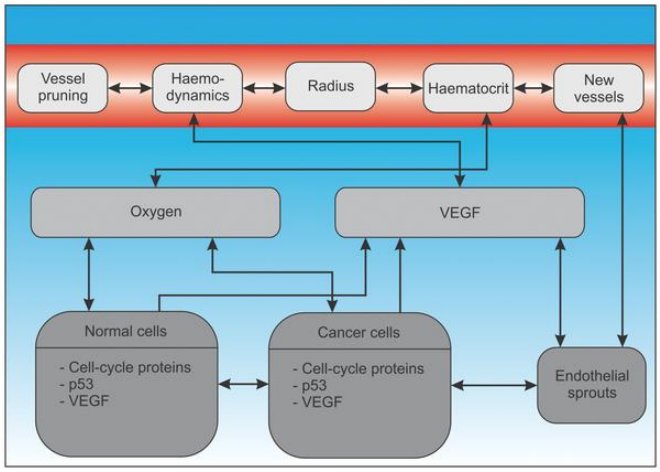

Figure 1: Multiscale model overview (interaction diagram). *This figure shows the connections between the different modelling layers. In the subcellular layer the cell cycle protein concentrations and the p53 and VEGF concentrations are modelled via systems of coupled ordinary differential equations. The local external oxygen concentration influences the duration of the cell cycles. Cells consume oxygen, and produce VEGF in the case of hypoxia. Extracellular VEGF also influences the emergence of endothelial sprouts and their biased random walk towards hypoxic regions. If endothelial sprouts connect to other sprouts or the existing vascular network, new vessels form. Vessel diameter is influenced by the local oxygen concentration and flow-related parameters, such as pressure and wall shear stress. The vascular network delivers oxygen throughout the tissue.*

Our model is formulated on a regular grid that subdivides the simulation domain into lattice sites. Each lattice site can be occupied by several biological cells whose movement on the lattice is governed by reinforced random walks, and whose proliferation is controlled by a subcellular cell cycle model. The vascular network consists of vessel segments connecting adjacent nodes on the lattice, with

defined inflow and outflow nodes with prescribed pressures. We also specify the amount of haematocrit entering the system through the inlets. The vessel network evolves via (i) sprouting of tip cells with a probability that increases with the local VEGF concentration, (ii) tip cell movement is described by a reinforced random walk, and (iii) new connections forming via anastomosis. In addition, vessel segments with low wall shear stress may be pruned away. Elliptic reaction-diffusion equations for the distributions of oxygen and VEGF are implemented on the same spatial lattice using finite difference approximations, and include source and sink terms based on the location of vessels (which act as sources of oxygen and sinks of VEGF) and the different cell types (e.g. cells act as sinks for oxygen and hypoxic cells as sources of VEGF).

In summary, after initialising the system, the diffusible fields, cellular and subcellular states are updated (including cell division and movement), before the vessel network is updated, this process being repeated until the simulation ends.

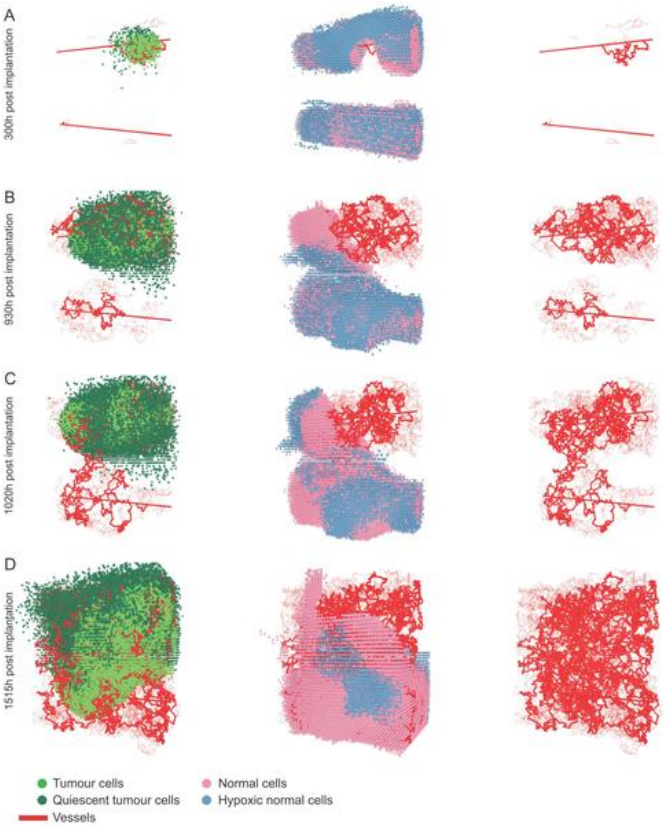

Figure 2: Tumour growth in healthy tissue. *The tumour cells and vasculature are depicted in the left column, the vasculature and normal cells in the middle column and the vessel network in the right column. The figure shows a realisation of a 50 x 50 x 50 domain with a cube of tumour cells implanted in healthy tissue with two straight initial vessels.*

The results from a typical simulation showing the development of a tumour and its associated network of blood vessels are depicted in Figure 2. Simulations were performed on a 50 x 50 x 50 lattice with spacing 40μm, which corresponds to a 2mm x 2mm x 2mm cube of tissue. For the following simulations, each lattice site can be occupied by at most one cell (either normal or cancerous), which implies that, for the grid size used (40μm), the tissue is loosely packed. A small tumour was implanted at t=0 in a population of normal cells perfused by two parallel parent vessels with countercurrent flow (i.e. the pressure drops and hence flows are in opposite directions). Initially, insufficient nutrient supply in unvascularised areas causes widespread death of the normal cells. The surviving tumour cells reduce the p53 threshold for death of normal cells, which further increases the death rate of the normal cells and enables the tumour to spread. Initially, most of the tumour cells are quiescent and secrete VEGF which stimulates an angiogenic response. After a certain period of time the quiescent cells die and only a small vascularised tumour remains encircling the upper vessel. The tumour expands preferentially along this vessel, in the direction of highest nutrient supply. Diffusion of VEGF throughout the domain stimulates the formation of new capillary sprouts from the lower parent vessel. When the sprouts anastomose with other sprouts or existing vessels, the oxygen supply increases, enabling the normal cell population to recover. Because the tumour cells consume more oxygen than normal cells, and they more readily secrete VEGF under hypoxia, VEGF levels are higher inside the tumour and the vascular density there is much higher than in the healthy tissue. The tumour remains localised around the upper vessel until new vessels connect the upper and lower vascular networks. Thereafter the tumour cells can spread to the lower region of the domain until eventually the domain is wholly occupied by cancer cells and their associated vasculature.

As a further step we document first results of a vascular tumour growth simulation for which the initial vascular geometry was taken from multiphoton fluorescence microscopy. The aim here is to integrate the mathematical model with *in vivo* experimental data. To generate experimental data on *in vivo* tumour vasculature, we implanted into a mouse dorsal window chamber a tumour construct comprising a central core of human breast cancer cells surrounded by rat microvessel fragments, embedded in a collagen matrix. The cancer cells and rat microvascular cells express different fluorescent proteins so that, following implantation, the tumour and its vascular network can be visualised.

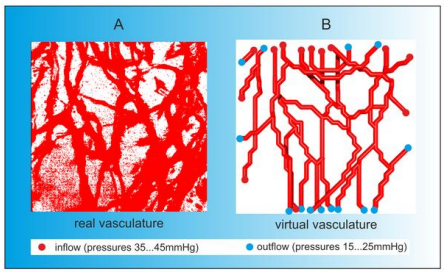

Figure 3: Image reconstruction. *We reconstructed the vascular network by applying the following strategy. 3D multiphoton fluorescence microscopy images (A) taken from mouse models in vivo formed the basis of our geometrical reconstruction. These images were transferred to OpenInventor and Matlab for image analysis. Based on the data we reconstructed the vascular graph model that describes the connectivity of the vascular network. B) We assigned inflow (red points) and outflow nodes (blue points) at various pressures in order to obtain a persistent and stable network. The vascular graph is characterised by the spatial coordinates of the nodes and the connections between them.*

We used the experimental data to reconstruct the vascular graph model, locating nodes in the vessel centres and connecting them by edges. We use this example principally as proof-of-concept. First, we embed the vascular system into healthy tissue and then simulate vessel adaptation until a steady-state is reached.

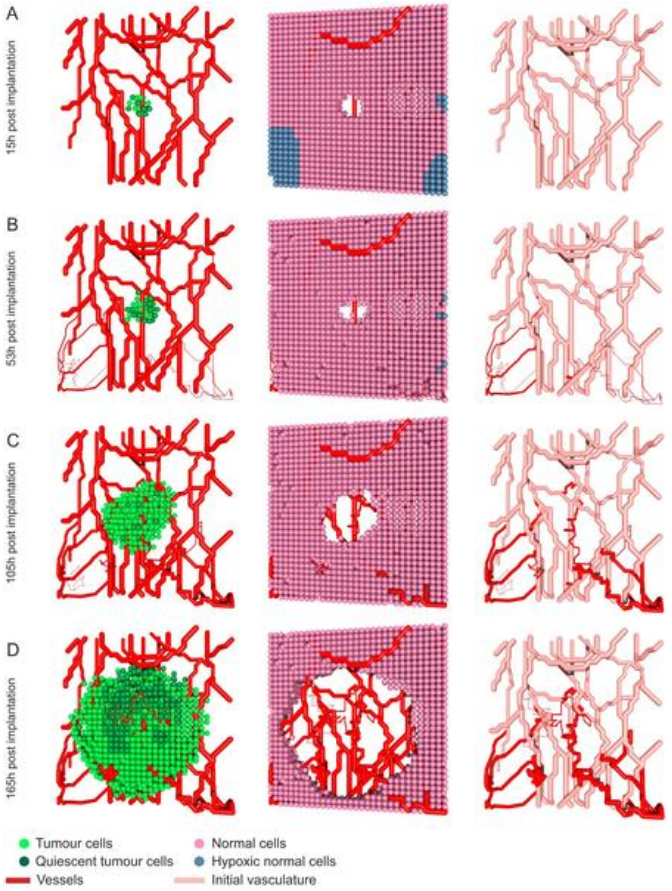

Figure 4: Proof-of-concept: tumour growth in an experimentally derived vascular network. *A)–D) show the temporal evolution of a tumour in a real vascular network embedded in normal tissue. As initial condition we have taken a vascular network from multiphoton fluorescence microscopy and embedded it in a 50 x 50 x50 cellular automaton domain. In the first column the tumour expands radially, and degrades the healthy tissue (second column). The predicted adaptations of the vascular system are shown in the third column where the experimentally derived network is shown in light red, while the new vessels are coloured in red.*

Currently in the models the vasculature is embedded in a healthy tissue into which a small tumour is implanted and its evolution is studied. A projection of a 3D image set of the tissue is presented in Figure 3. In Figure 4 we observe that the tumour expands radially into the surrounding healthy tissue which is degraded by the cancer cells by decreasing the p53 death-threshold for normal cells. Normal cells in the lower left and right corners of the simulation domain (first column) are exposed to low oxygen (hypoxia), and hence produce VEGF which induces an angiogenic response in our model. While the new vessel in the lower left corner is persistent and increases in radius, the vessel in the lower right corner is pruned back. In this case pruning occurs because the new blood vessel connects vessels from the initial network that have similar pressures. In general it can be said that the normal cells are adequately nourished by oxygen as only a few hypoxic cells can be observed in simulations with normal cells only. In contrast, we find a high percentage of quiescent cancer cells in all states of tumour growth, leading to further angiogenesis in our simulations (see Figure 4). The dark red vessels in row 3 indicate new vessels that develop after tumour implantation. In conclusion, our model predicts an increase in the vascular density following tumour implantation.